(43) D. A. MacInnes, J. Polym. Sci., 15, 657 (1977).
(44) D. Pugh and D. A. Jones, Polymer, 19, 1008 (1978).
(45) M. A. Cochran, J. H. Dunbar, A. M. North, and R. A. Pethrick, J. Chem. Soc., Faraday Trans. 2, 70, 215 (1974).
(46) H. Nomura, S. Kato, and Y. Miyahara, Nippon Kagaku Kaishi, 1554 (1973).
(47) A. M. North, R. A. Pethrick, and I. Rhoney, J. Chem. Soc., Faraday Trans. 2, 70, 223 (1974).

Calculation of the High-Pressure Phase Diagram of Polyethylene

Richard G. Priest

Naval Research Laboratory, Washington, D.C. 20375. *Received November 7, 1984*

ABSTRACT: The pressure–temperature phase diagram of polyethylene is distinguished by a partially ordered phase which interposes between the melt and orthorhombic crystal for pressure greater than 3.5 kbar. This phase, called the high-pressure intermediate phase (HPIP), is characterized by a hexagonal lattice of highly extended chains. Despite the high extension of the chains, rotational fluctuations about the single bonds are significant. This paper is a calculation of the phase boundary between the crystal and HPIP phases. The latent heat of the first-order crystal–HPIP phase transition is also calculated. Elements of the model are entropy and energy associated with the rotations about the single bonds and the energy associated with interchain interaction. Treatment of the bond rotational degrees of freedom is based on the distribution function calculated in an earlier publication. The remaining degrees of freedom are considered in a simple potential energy approximation. The results for the location and slope of the phase boundary are in good agreement with experiment. The calculated values of the latent heat and volume discontinuity of the phase transition fall between the experimental values recorded in the two literature data sets.

I. Introduction

The phase diagram of polyethylene at high pressure has been the subject of a number of experimental investigations.[1-3] The most important feature of this phase diagram is the extent of the domain of stability of the high-pressure intermediate phase (HPIP). This phase, for which the generic nomenclature "condis crystal" has been suggested,[4] interposes between the melt and the orthorhombic crystal for pressures greater than 3.5 kbar. In the HPIP, the polymer chains are very highly extended and oriented. The phase is hexagonal with the chain axes along the unique direction. Although the structure is apparently well ordered, the thermodynamic data indicate that there is a fair amount of dihedral angle disorder in the HPIP. The physical picture is that while in the crystal the fluctuations of the bond rotations away from the trans position are small, in the HPIP the fluctuations in these rotations are significant. In two earlier papers[5,6] a model calculation for this dihedral angle disorder was developed. This model is based on the idea that the structural effect of the interchain interactions is to confine a polymer chain to a cylindrical cavity of infinite length and fixed cross-sectional area. The entropy associated with dihedral angle disorder can be calculated as a function of the cross-sectional area on the basis of this model. While this approach is capable of obtaining the magnitude of the discontinuity in entropy at the HPIP–orthorhombic phase transition, it must be augmented by a model of the interchain energetics in order to form the basis for a full calculation of the phase boundary between the HPIP and the orthorhombic crystal. The calculation of the interchain energetics and of the HPIP–orthorhombic phase boundary is the subject of this paper. The approach used here is based on an analysis of the equation of state of crystalline polyethylene by Pastine.[7] The augmented calculation is the first statistical mechanical analysis of the HPIP. Earlier theoretical work[8-10] has been confined to thermodynamic phenomenology.

The calculation of this paper draws on numerical results contained in ref 5–7. These numerical results are parameterized by quantities related to the cross-sectional area per chain. In order to make the presentation of this paper as straightforward and self-contained as possible, all of the required numerical results are brought into the form of analytic functions of the same parameter. This parameter is R, the radius of the cylinder confining the skeleton of the polymer chain divided by the length of the carbon–carbon bond. In order to do this, the numerical results which appear in tabular or graphical form are fit to simple analytic functions of R.

This approach has the merit that all of the contributions to the free energy appear as simple functions of R. It is then an easy matter to minimize the free energy with respect to R. It is found that for a certain range of values of the temperature and pressure, there are two minima of the free energy as a function of R. One minimum corresponds to the HPIP, and the other to the orthorhombic crystal. There should be a third minimum corresponding to the melt phase. However, the method of calculation used in ref 6 does not allow calculation of the dihedral angle entropy in the region of R appropriate to the melt phase. Consequently the results of this calculation are limited to the calculation of the HPIP–orthorhombic crystal phase boundary. The calculated slope of this boundary and its intercept with the experimentally determined phase boundary of the melt phase are in excellent agreement with experiment.

The organization of this paper is as follows. Section II discusses the parameterization of the free energy and the dihedral angle distribution function in terms of R. This section also discusses how the numerical results of ref 5 and 6 are incorporated. Section III is concerned with the contribution due to the degrees of freedom external to the chain. Results and conclusions are presented in section IV.

II. Parameterization of Statistical Quantities in Terms of R

A. Free Energy. The Gibbs free energy, G, of the polymer chain may be thought of as the sum of five contributions. The first is the average van der Waals energy associated with interchain interaction, E_0. This contri-

bution depends on the specific volume per CH_2 group, V. The second contribution is the explicit pressure × volume, PV, term. The third and fourth contributions are associated with the dihedral angle degrees of freedom treated in ref 5 and 6. The third is the energetic part as calculated from the Scott–Scheraga potential averaged over the dihedral angle distribution. The fourth is the entropic contribution associated with the dihedral angle disorder specified by the distribution function. For the evaluation of these last two terms, the dihedral angle distribution function calculated in ref 6 will be used. The distribution function depends on the parameter R and therefore implicitly on the specific volume. The fifth contribution, D, is the Debye energy and entropy associated with all the remaining internal degrees of freedom of the polymer chains. To a very good approximation this contribution to the free energy depends only on the temperature, T, and not on the specific volume. The sum of these five contributions can be expressed as

$$G(P,T) = E_0(V) + PV + E_{SS}(R) - TS_D(R) + D(T) \quad (1)$$

The extensive quantities, G, V, E_0, E_{SS}, S_D, and D, are defined on a mole of CH_2 basis. in eq 1, the Scott–Scheraga energy term, E_{SS}, and the dihedral entropy term, S_D, are expressed as functions of R. This parameter is related to V as will be discussed below.

The conventional approach to the analysis of an expression like that of eq 1 is to find the minima of G with respect to V for fixed P and T. In this work I take the somewhat different but equivalent approach of locating minima of G with respect to R. In order to do this the relation between V and R, $V(R)$, must be found. It is also necessary to obtain an expression giving the parameterization of the dihedral angle distribution function by R. The next two subsections deal with these relationships.

B. Dihedral Angle Distribution Function. The most important internal degrees of freedom for the calculation of the phase diagram are those associated with the dihedral angles, that is, the rotations about the single bonds. To the level of approximation used in ref 6, the thermodynamic quantities of interest can be calculated from the dihedral angle distribution function. In particular, averages of functions of the dihedral angle are equal to integrals weighted by this distribution function. In ref 6 the dihedral angle distribution function was calculated by an integral equation method. Two models were considered. The first was an athermal situation for which the Scott–Scheraga type dihedral angle potential was neglected. The only interaction in this model is the confinement of the chain backbone to a cylinder of radius R. The result for the dihedral angle distribution function for this model can be expressed in the form

$$\begin{aligned} h_0(\alpha) &= (1 - |\alpha|/\alpha_{max})/\alpha_{max}, \quad |\alpha| < \alpha_{max} \\ &= 0, \quad |\alpha| > \alpha_{max} \end{aligned} \quad (2)$$

where h_0 is the distribution function, α is the dihedral angle excursion from the trans configuration, and α_{max} is the effective maximum value of α consistent with confinement to a cylinder of radius R. The detailed calculation yielded numerical values for α_{max} as a function of R. For R in the physically interesting range, $0.36 < R < 0.7$, the numerical results, shown in Figure 2 of ref 6, can be fit to the form

$$\alpha_{max} = 3(-0.370 + 1.79R) \quad (3)$$

The thermal model, for which the Scott–Scheraga dihedral angle potential is included in addition to the interactions of the athermal model, cannot be rigorously analyzed in the same fashion as the athermal model. Instead an approximation for the distribution function is introduced. The approximate form is a product of the form of eq 2 and the Boltzmann weight appropriate to the dihedral angle potential.

$$h(\alpha) = Zh_0(\alpha) \exp(-V_{SS}/k_BT) \quad (4)$$

where Z is a normalization constant, k_B is Boltzmann's constant, and V_{SS} ($=V_{SS}(\alpha)$) is the three-well (one trans and two gauche) potential given in ref 11. This distribution function can be used to evaluate E_{SS} and S_D and to calculate average dihedral angle excursions:

$$E_{SS} = N_0 \int h(\alpha) V_{SS}(\alpha)\, d\alpha \quad (5)$$

$$S_D = -N_0 k_B \int h(\alpha) \ln (h(\alpha))\, d\alpha \quad (6)$$

where N_0 is Avogadro's number. Equation 6 is an approximation which assumes that the joint dihedral angle distribution function is separable into a product of the single-angle distribution functions. A unimportant constant addition to the free energy is introduced by eq 6 by virtue of the measure of the angular unit (degrees or radians).

C. Specific Volume. As discussed above, it is desirable to obtain an analytic form for the relation between R and V. Since V is proportional to the product of the cross-sectional area per chain, A, and the average projection onto the c axis of the CH_2 repeat group, L, each of these quantities must be given as a function of R. This is relatively easy to do in the case of A. As argued in ref 6, changes in A are proportional to changes in R and not to R^2 due to nesting of the chains. Equation 28 of ref 6 states this relation in the form

$$\Delta A = \Delta R d_0 d_{CC} \quad (7)$$

where d_0 is a length on the order of the diameter of the cylindrical cavity occupied by a chain and d_{CC} is the length of the carbon–carbon bond. It is straightforward to generalize this result in order to give an analytic function for the area. This generalization is

$$A = A_0 + (R - 0.288) d_0 d_{CC} \quad (8)$$

where A_0 is the cross-sectional area of the chain in the crystal at low temperature. The number 0.288 represents the smallest value of R that will accommodate the zigzag polymer backbone. Numerical values can easily be assigned to A_0, d_0, and d_{CC}. From X-ray[1] data $A_0 = 17.53$ Å^2 and $d_{CC} = 1.54$ Å. To get the best results for A for the range of R of most interest, $0.38 < R < 0.7$, the value of d_0 is chosen to be 4.77 Å. A circle of this diameter has an area of 17.88 Å^2. This is the area of the crystal just at the melting line at a pressure of about 5 kbar. For the value of R corresponding to the crystal at high pressure, $R = 0.38$, and for the value corresponding to the intermediate phase, $R = 0.68$, eq 8 gives good agreement with the experimental areas for the crystal and HPIP, respectively.[1]

The analysis of the variation of L with R is more complex. It is obvious that dihedral angle disorder will bring about a reduction of this length from its maximum value $L_0 = (2/3)^{1/2} d_{CC}$. This maximum value is found in the perfectly ordered crystal at low temperature. Elementary geometric considerations can be used to show that $1 - L/L_0$ is quadratic in dihedral angle excursions away from the all-trans conformation. In light of this result it is reasonable to expect that

$$1 - L/L_0 = a\langle\alpha^2\rangle \quad (9)$$

where $\langle\alpha^2\rangle$ is the average of the square of the dihedral angle excursion and a is a constant. This is indeed the case to a very good approximation. Figure 6 of ref 6 presents

a numerical relationship between $1 - L/L_0$ and R calculated from the athermal model. Since the athermal model result for $\langle\alpha^2\rangle$ ($\equiv\langle\alpha^2\rangle_0$) can be easily calculated from eq 2, it is possible to obtain a relationship between $1 - L/L_0$ and $\langle\alpha^2\rangle_0$ by eliminating R. The result obtained from the distribution of eq 2 is

$$\langle\alpha^2\rangle_0 = 1.5(-0.370 + 1.79R)^2 \quad (10)$$

When this is combined with the data of Figure 6 of ref 6, a very simple form emerges:

$$1 - L/L_0 = 0.0822\langle\alpha^2\rangle_0 \quad (11)$$

This result actually holds very well even for small values of $(R - 0.288)$, where eq 3 is not valid. This was checked by using the numerical results for α_{max} from Figure 2 of ref 6. Equation 11 is strictly valid for the athermal model only. However, the origin of eq 11 is essentially geometric. Thus it is a reasonable approximation to use it with $\langle\alpha^2\rangle$ calculated from the thermal model. The average $\langle\alpha^2\rangle$ depends on both R and T. However, for fixed R the dependence on T in the range of interest, 490 K < T < 530 K, is not strong. For this reason it may be evaluated at T = 500 K as a function of R. The result may be cast in the analytic form of a power series in $(R - 0.288)$.

$$\langle\alpha^2\rangle = 1.14(R - 0.288) - 8.16(R - 0.288)^2 + 24.51(R - 0.288)^3 \quad (12)$$

This form may be combined with eq 11 to obtain

$$1 - L/L_0 = 0.093(R - 0.288) - 0.670(R - 0.288)^2 + 2.01(R - 0.288)^3 \quad (13)$$

The least-squares fitting procedure was used in obtaining the coefficients in eq 11–13. The expansions are valid for $R < 0.7$. Equations 8 and 13 give V as a function of R.

III. Interchain Interaction

The important interchain interactions are repulsion between nonbonded hydrogens and van der Waals attraction between CH_2 groups. A method for calculating these energies for the case of the polymer crystal has been developed by Pastine.[7] Pastine's work had as its objective the calculation of the equation of state for the crystal. Several results obtained in this work are of relevance here. First, it was found that the interchain interactions can be viewed as a function of a single structural parameter, x, over a wide range of pressures. The parameter x is effectively the ratio of the cross-sectional area per chain to its value at the absolute zero of temperature:

$$x = A/A_0 = (A_0 + (R - 0.288)d_0d_{CC})/A_0 \quad (14)$$

Second, the interactions can be represented in a simple form through consideration of the internal pressure, $P^c(x)$. At T = 0, this is the pressure that must be overcome to compress the crystal. It is zero for x = 1 and positive for $x < 1$. For $x > 1$, P^c is negative, indicating that interchain interactions tend to draw the chains together so long as $x > 1$. In ref 7, P^c is given in graphical and tabular form as a function of x. The form of this relationship is very well fit by a Pade function of the form

$$P^c(x) = \frac{-C(x - 1)}{1 + B(x - 1)} \quad (15)$$

When C is chosen to give the correct slope at x = 1 and B is chosen to give the best fit to the tabular data, the parameter values are C = 130 kbar and B = 3.47. To expand the cross-sectional area from A_1 to A_2, work must be done against P^c. The energy associated with this work is E_0 of eq 1. It is given by

$$E_0 = N_0\int_{A_1}^{A_2} P^cL_0\,dA \quad (16)$$

The fact that L_0 and not L enters here is due to the way P^c is calculated in ref 7. The unit cell c-axis length is twice L_0; thus from the X-ray data, L_0 = 1.27 Å. As mentioned in the Introduction, it is convenient to express energies such as E_0 in terms of the parameter R. This is easily done by changing the integration variable in eq 16.

$$E_0 = N_0L_0\int_{R_1}^{R_2} P^c(R)\frac{dA}{dR}\,dR \quad (17)$$

$$E_0(R) = K\int_{R_1}^{R_2} P^c(R)\,dR$$

with $K = N_0L_0d_0d_{CC}$ = 560 J/kbar. This integral is evaluated by using the relationship between R and x given by eq 14. The fact that eq 17 gives E_0 = 0 at $R = R_1$ means that this energy has been specified up to a constant. This is not important since additive constants have no significance in eq 1.

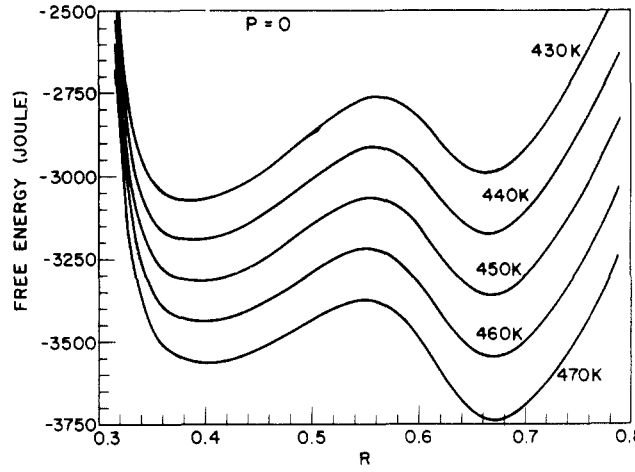

Figure 1. Molar Gibbs free energy as a function of R for atmospheric pressure. Temperature in kelvin is indicated. The zero of the free energy scale is not significant.

IV. Results and Conclusion

The development of the previous two sections gives the dependence of each of the contributions to the free energy, except the Debye contribution, on R. It is assumed that the Debye contribution, $D(T)$ is independent of R. $E_0(R)$ is given by eq 17, 15, and 14. The PV contribution can be obtained from eq 8 and 13. E_{SS} is given[12] by eq 5, 4, 2, and 3. S_D is given[12] by eq 6, 4, 2, and 3. Using these results, one may numerically determine, as a function of R, the Gibbs free energy per mole, G. A curve may be generated for any specified values of the two intensive thermodynamic variables, the temperature, T, and the pressure, P.

Figures 1–3 show examples of these types of curves. As discussed above, the zero of the free energy is arbitrary due to unimportant additive constants. Each curve has two local minima, one corresponding to the crystal at approximately R = 0.38, and the other corresponding to the HPIP at approximately R = 0.67. One of the two local minima is the global minimum of the free energy. The state, crystal or HPIP, corresponding to the global minimum is the equilibrium state at the specified values of P and T. At certain values of the parameters P and T, the values of the free energy at the two minima are equal.

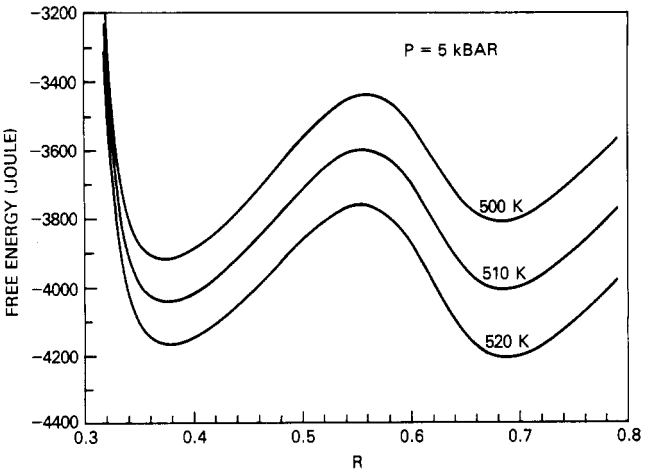

Figure 2. Molar Gibbs free energy as a function of R for 5-kbar pressure. The phase transition occurs at 514 K.

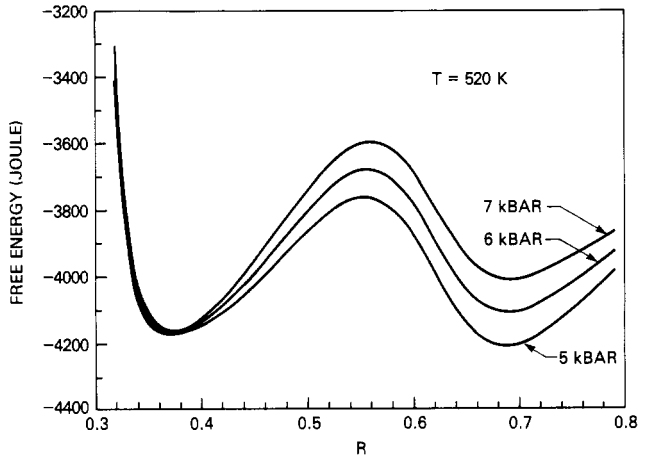

Figure 3. Molar Gibbs free energy as a function of R with the temperature fixed at 520 K. Results for three values of the pressure are shown.

These points are on the phase boundary line separating the crystal and HPIP in the P,T phase diagram. By calculating a number of curves such as those shown in Figures 1–3, it is thus possible to construct this phase boundary in the P,T plane. The result is shown in Figure 4. Also shown in Figure 4 is the experimental result[3] for the boundary of the melt phase. As explained above, this boundary cannot be calculated by using the approach used in this paper and in ref 6. It is included in Figure 4 so that an appreciation of the location of the triple point, where the melt, crystal, and HPIP coexist, can be obtained. There are two data sets which systematically cover a range of pressures.[2,3] Data points from these references are included in Figure 4 to indicate the degree of agreement between the theoretical result obtained here and the data. As can be seen from the figure, there is a good agreement with both the slope and the intercept with the melt boundary.

Once the phase boundary has been located, it is a straightforward matter to calculate the latent heat of the first-order phase transition. At a point on the phase boundary, the free energy evaluated at the two minima of $G(R)$ is the same. The latent of the transition is equal to $T\Delta S_D$, where ΔS_D is the difference in S_D as evaluated at the values of R corresponding to the two minima. The result for ΔS_D is presented in Figure 5 together with the data from ref 2 and 3. The calculated curve agrees fairly well with the data sets if the last point from ref 2 is ignored. The magnitude of the theoretical result is in satisfactory

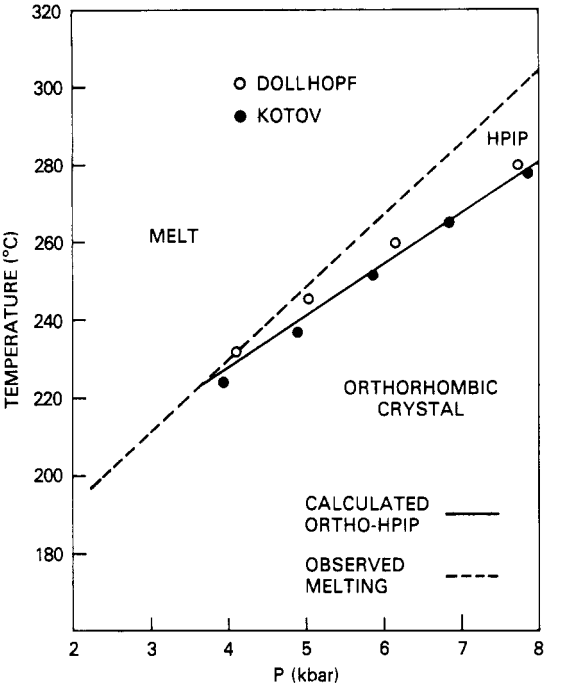

Figure 4. Phase diagram of polyethylene. The orthorhombic, melt, and HPIP regions are indicated. Dashed line is the observed melting transition.[3] Solid line is the calculated result for the orthorhombic–HPIP phase boundary. Circles are measured points on this boundary. Solid circles are data from ref 3, and open circles are data from ref 2. Both data sets are reviewed in ref 1.

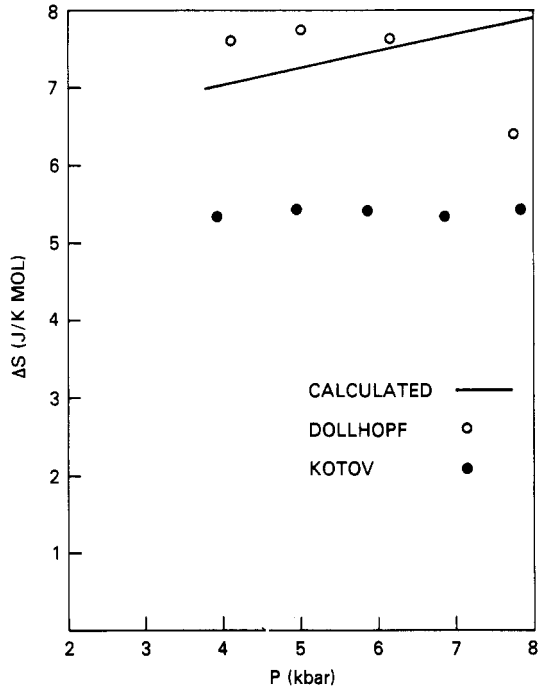

Figure 5. Change in entropy at the orthorhombic–HPIP phase transition. Solid curve is the calculated result. Open circles are data from ref 2, and solid circles are data from ref 3.

agreement with experiment, considering the discrepancy between the two data sets, but the calculated slope is evidently too large. The simple model of the energetic contribution to the free energy considered here cannot produce the correct value of this slope. However, the fact that the value of this slope is small is correctly predicted.

The change in volume at the phase transition is related to ΔS_D by the Clausius–Clapeyron equation. In fact, it is the volume change which is directly measured. Using the

value 13.1 K/kbar for dT/dP (see Figure 4) and the values of ΔS_D from Figure 5, the theoretical value of the volume discontinuity at the phase transition is calculated to range from 0.066 cm^3/g at $P = 4$ kbar to 0.074 cm^3/g at $P = 8$ kbar. As with the entropy discontinuity, the numerical values of the volume discontinuity are in general agreement with experiment, while the slight increasing trend with pressure is not. The experimental values from ref 2 center about 0.069 cm^3/g and those of ref 3 cluster about 0.056 cm^3/g. In both data sets there is evidence of a slight decreasing trend with increasing pressure. The source of the incorrectly predicted slope is the too large slope of ΔS_D mentioned above.

In summary, the model of the energetic contributions to the free energy of polyethylene presented here can be used to augment the model of the entropic part of the free energy which was presented in ref 6. The result is a complete model of the HPIP. The model correctly predicts the essential features of the orthorhombic–HPIP phase transition.

Most of the earlier theoretical work on the HPIP has been confined to thermodynamic modeling. Bassett and Turner[9] deduced the schematic form of the free energy–temperature phase diagram from very general considerations. This line of investigation was advanced by Asai,[10] who employed thermodynamic arguments to predict the pressure dependence of the free energy. Additional analysis of this type can be found in ref 1. This type of theoretical approach makes use of thermodynamic data that must be taken from experiment. Consequently it cannot provide a complete theoretical description of the HPIP. A complete theory of the phase transition must employ a statistical mechanical approach. The author is aware of only three calculations predating the present work (including ref 5 and 6). The earliest is a calculation by Hoffman[8] which is based on consideration of rigid rotation of chains about their axes. Current structural information makes it clear that this model is not correct. The same is true of calculations by Pechhold et al.[13] The kink block model of this reference envisions the chain shortening which accompanies the phase transition as being due to large numbers of trans–gauche–trans–gauche kink block sequences. X-ray structural data[14] are inconsistent with such a highly correlated defect (relative to the all trans) structure. Finally, the statistical analysis of Yamamoto[14] is useful for determining the nature and frequency of occurrence of the structural defects. However, the analysis of this reference relies on detailed X-ray measurements and so is not a first-principles calculation. Further, it does not make connection with the thermodynamic data.

The calculation of this paper (and ref 6) is a statistical mechanical calculation which does not rely on any thermodynamic data specific to the HPIP. It successfully predicts the main thermodynamic properties of the orthorhombic–HPIP phase transition. The structural defects which it considers are consistent with the known structural data.

Registry No. Polyethylene (homopolymer), 9002-88-4.

References and Notes

(1) The most recent review is: Leute, U.; Dollhopf, W. *Colloid Polym. Sci.* **1980**, *258*, 353.
(2) Dollhopf, W. Ph.D. Thesis, Ulm, 1979.
(3) Kotov, N.; Zubov, Y.; Bakeyev, N. *Dokl. Akad, Nauk SSSR* **1976**, *229*, 1375.
(4) Wunderlich, B.; Grebowicz, J. *Adv. Polym. Sci.*, in press.
(5) Priest, R. *J. Appl. Phys.* **1981**, *52*, 5930.
(6) Priest, R. *Macromolecules* **1982**, *15*, 1357.
(7) Pastine, D. J. *J. Chem. Phys.* **1968**, *49*, 3012.
(8) Hoffman, J. D. *J. Chem. Phys.* **1952**, *20*, 541.
(9) Bassett, D. C.; Turner, B. *Philos. Mag.* **1974**, *29*, 925.
(10) Asai, K. *Polymer* **1982**, *23*, 391.
(11) Scott, R. A.; Scheraga, H. A. *J. Chem. Phys.* **1967**, *44*, 3054.
(12) The numerical values for α_{max} are used for $R < 0.38$.
(13) Pechhold, W.; Liska, E.; Grossmann, H. P.; Hagele, P. C. *Pure Appl. Chem.* **1976**, *46*, 487.
(14) Yamamoto, T. *J. Macromol. Sci., Phys.* **1979**, *B16*, 487.

Notes

Monte Carlo Simulation of Polymerization with Reversible Chain Transfer

KENNETH F. O'DRISCOLL

Department of Chemical Engineering, University of Waterloo, Waterloo, Ontario N2L 3G1, Canada.

Received November 28, 1984

In a recent paper,[1] Szwarc and Zimm have shown that the model which represents the experimental work of Kennedy et al.[2] (Scheme I) can be represented by a set of differential equations which they solved numerically.

In Scheme I, initiator HA reacts reversibly with monomer, P_1, or dead polymer, P_n, to form live polymer $HR_n^+A^-$; the latter species propagates by irreversible addition of monomer; its loss of HA when $n > 1$ is in effect a spontaneous chain transfer.

Scheme I

$$HA + P_n \underset{k_{-1}}{\overset{k_1}{\rightleftharpoons}} HR_n^+A^-$$

$$HR_n^+A^- + P_1 \xrightarrow{k_p} HR_n^+A^-$$

Some difficulty was experienced in the numerical solution of the model on a VAX 11-780 because of the equations' stiffness;[1] further tests of the authors' conclusions were restricted by the magnitude of the variables needed in the numerical differential equation solution. Even so they were able to establish conclusively some rather interesting points about the kinetics of Scheme I. One of these concerned the polydispersity of the molecular weight distribution $R = \bar{P}_w/\bar{P}_n$, which was expected to approach $^4/_3$ at long times; the value of $^4/_3$ was arrived at by deduction from an analytical solution possible for long times. However, the computer solution indicated the polydispersity approaching what might be a maximum at $R = 1.5$; long-time solutions, where R might approach $^4/_3$, were not possible with the resources available. An unexpected (and unexplained) behavior of the R vs. time plot was a hump at short times, which was seen in more than one calculation.

There are essentially two ways to solve the kinetics of a polymerization model: one is to solve differential equations, analytically or numerically, and the other is to use Monte Carlo simulations. Either method requires the same input information and is capable of producing the

0024-9297/85/2218-1508$01.50/0